



ORIGINAL ARTICLE

Biological and chemical sulfide oxidation in a *Beggiatoa* inhabited marine sediment

André Preisler, Dirk de Beer, Anna Lichtschlag, Gaute Lavik, Antje Boetius and Bo Barker Jørgensen

Department of Biogeochemistry, Max-Planck-Institute for Marine Microbiology, Bremen, Germany

The ecological niche of nitrate-storing *Beggiatoa*, and their contribution to the removal of sulfide were investigated in coastal sediment. With microsensors a clear suboxic zone of 2–10 cm thick was identified, where neither oxygen nor free sulfide was detectable. In this zone most of the *Beggiatoa* were found, where they oxidize sulfide with internally stored nitrate. The sulfide input into the suboxic zone was dominated by an upward sulfide flux from deeper sediment, whereas the local production in the suboxic zone was much smaller. Despite their abundance, the calculated sulfide-oxidizing capacity of the *Beggiatoa* could account for only a small fraction of the total sulfide removal in the sediment. Consequently, most of the sulfide flux into the suboxic layer must have been removed by chemical processes, mainly by precipitation with Fe^{2+} and oxidation by Fe(III), which was coupled with a pH increase. The free Fe^{2+} diffusing upwards was oxidized by Mn(IV), resulting in a strong pH decrease. The nitrate storage capacity allows *Beggiatoa* to migrate randomly up and down in anoxic sediments with an accumulated gliding distance of 4 m before running out of nitrate. We propose that the steep sulfide gradient and corresponding high sulfide flux, a typical characteristic of *Beggiatoa* habitats, is not needed for their metabolic performance, but rather used as a chemotactic cue by the highly motile filaments to avoid getting lost at depth in the sediment. Indeed sulfide is a repellent for *Beggiatoa*.

The ISME Journal (2007) 1, 341–353; doi:10.1038/ismej.2007.50; published online 28 June 2007

Subject Category: geomicrobiology and microbial contributions to geochemical cycles

Keywords: microsensor; chemotaxis; geochemistry; suboxic zone; sulfate reduction; nitrate reduction

Introduction

Beggiatoa are multicellular, filamentous, colorless sulfur bacteria of the γ -proteobacteria clade, inhabiting freshwater, marine and hypersaline sediments and forming distinct white mats. The large marine sulfide oxidizers *Beggiatoa* and *Thioploca*, with filament diameters $> 10 \mu\text{m}$, and *Thiomargarita*, can all store nitrate in vacuoles (Fossing *et al.*, 1995; Schulz *et al.*, 1999) up to a concentration of 370 mM (McHatton *et al.*, 1996; Ahmad *et al.*, 1999). In sediments containing *Beggiatoa*, total nitrate concentrations can be orders of magnitude higher than in the overlying seawater due to intracellular storage (Sayama, 2001; de Beer *et al.*, 2006). This intracellular nitrate is used to oxidize sulfide in deeper anoxic zones of sediments. The oxidation most probably proceeds via dissimilatory nitrate reduction to ammonium (DNRA) (Vargas and Strohl, 1985; McHatton *et al.*, 1996; Schulz and Jørgensen, 2001; Sayama *et al.*, 2005). Sulfide is oxidized first to

elemental sulfur (Nelson *et al.*, 1986) and stored in globules that give the mats a white appearance. In a second step, the sulfur is further oxidized to sulfate (Otte *et al.*, 1999).

Beggiatoa inhabits strongly reduced, organic-rich or hydrocarbon-rich, porous sediments, with sufficient interstitial space for motility (Jørgensen, 1977). Commonly, the oxic and sulfidic zones are separated by a zone where neither is present in measurable concentration ($\leq 1 \mu\text{M}$), further called the suboxic zone (Froelich *et al.*, 1979; Berner, 1981). *Beggiatoa* is thought to be a cause of the separation, because of its abundance and its capacity to anaerobically oxidize sulfide with nitrate (Sayama *et al.*, 2005). Indeed, up to 20 g *Beggiatoa* biomass per m^2 was found in Limfjorden (Jørgensen, 1977). A more classical explanation for the suboxic zone is chemical sulfide oxidation with Fe(III) as electron acceptor. Fe(III) is rapidly formed by oxidation of Fe^{2+} with oxygen. As Fe(III) is insoluble, it needs to be transported into the suboxic zone by sediment reworking, for example by bioturbation or by hydrodynamics. Both the transport rate and the specific reactivity of Fe(III)-bearing minerals can limit the chemical oxidation of sulfide in sediments (Canfield, 1989).

Thus, sulfide oxidation by *Beggiatoa*, or other sulfur bacteria, may compete with chemical oxida-

Correspondence: Dr D de Beer, Max-Planck-Institute for Marine Microbiology, Celsiusstrasse 1, Bremen, Germany.

E-mail: dbeer@mpi-bremen.de

Received 28 March 2007; revised and accepted 31 May 2007; published online 28 June 2007

tion. In Limfjorden sediments, *Beggiatoa* can oxidize 50% or more of the produced free sulfide (Jørgensen, 1977; Mussmann *et al.*, 2003). Experimental studies showed that *Thioploca* communities off the coast of Chile have the potential to oxidize 25–91% of the free sulfide produced by sulfate reduction (Otte *et al.*, 1999). Field studies suggest that *Thioploca* can oxidize a maximum of 16–34% of sulfide production (Ferdelman *et al.*, 1997). The actual importance of nitrate-storing bacteria for the benthic sulfur cycle can thus vary strongly, whereas the contribution by chemical oxidation remains uncertain.

We studied the physiology and chemotactic responses of *Beggiatoa* to explain its role in the N and S conversions in their preferred habitat. We characterized sediments that are densely colonized by *Beggiatoa* using microsensors, we studied the metal chemistry in the *Beggiatoa* zone, and estimated the sulfide oxidation rates by *Beggiatoa* and by chemical processes.

Methods

Sampling

Sediments were sampled in cores with a diameter of 10 cm, using a small multiple corer (Barnett *et al.*, 1984), on four fieldtrips in 2002 and 2003 in Eckenförde Bay, Germany (54°31.30N, 10°02.18E and 54°31.15N, 10°01.28E) at a water depth of 25–28 m. A detailed description of the sampling site is published (Treude *et al.*, 2005). The sediments were transported to a laboratory near the sampling site (IfM-Geomar, Kiel, Germany), where the analyses were immediately started. The vertical distributions of the light (oxidized) and dark (reduced) zones were similar in parallel cores used for porosity, chemical analysis, biomass determinations and microsensor analyses. Cores that were not immediately used were stored at 15°C.

Microsensor measurements

Retrieved sediments. Microprofiles in retrieved sediment cores were measured within 3 days after sampling. The measurements were performed at 15°C. The overlying water was stirred gently by an air jet over the water surface. Profiles of nitrate plus nitrite were measured with a biomicrosensor (Larsen *et al.*, 1997), having a tip diameter of 100 μm and a 90% response time (t_{90}) of 2 min. Microsensors for O_2 , H_2S and pH were made and used as described previously (Revsbech, 1989; Jeroschewski *et al.*, 1996; de Beer, 2000). The tip diameters were ca. 10 μm , the $t_{90} < 3$ s. The microsensors were mounted on a motor-driven micromanipulator. Motor control and data acquisition were done using a computer. The position of the sediment surface was determined with a dissection scope. The total dissolved sulfide profiles were calculated from the measured H_2S and pH microprofiles (Jeroschewski

et al., 1996). The value for $\text{p}K_1$ (for the equilibrium between H_2S and HS^-) used was corrected for temperature and salinity (22‰) (Millero *et al.*, 1988).

In situ. The shafts of O_2 , H_2S and pH microsensors (three each) were elongated with 40 cm glass tubes, to a total length of 57 cm. The sensors were calibrated after mounting on a deep-sea profiler (Wenzhöfer *et al.*, 2000). The sensors were mounted on the bottom of the titanium housing within a horizontal distance of maximally 11 cm. The titanium housing, containing amplifiers and a computer for data acquisition and motor control, could be moved vertically by a spindle in a threading on the frame, with a smallest step size of 25 μm . The motor on top of the housing was connected directly to the spindle. The relative vertical positions of the sensor tips were carefully measured, so that the resulting profiles could be aligned. The profiler was pre-programmed to measure a vertical profile, with steps of 250 μm , over a depth of 50 cm. Each step included a waiting time of 4 s before a reading was made, consisting of the average of four samplings in a time interval of 4 s. The profiling started 2 h after deployment. The profiler was mounted on a frame and deployed with a winch.

For profile analysis, the surface was taken as reference point (depth = 0), defined by the steepest slope of the oxygen profile. From the *in situ* and *ex situ* measured steady-state sulfide profiles, we calculated the local diffusive fluxes, using Ficks law of diffusion ($J = D_s \text{d}C/\text{d}x$, with D_s the effective diffusion coefficient and $\text{d}C/\text{d}x$ the local gradients). D_s was calculated from the molecular diffusion coefficient (D_w), corrected for salinity and temperature (Li and Gregory, 1974) and the porosity (ϕ) (Ullman and Aller, 1982) using $D_s = \phi^2 D_w$, resulting in $8.3 \times 10^{-10} \text{ m}^2/\text{s}$ for sulfide at 15°C. Porosity was determined from the weight loss upon drying at 60°C for 72 h. The density was determined by weighing known volumes of sediment. The local sulfide conversion rates were obtained from reaction-transport calculations (Gieseke and de Beer, 2004). As no sulfide left the sediment, the sum of the local sulfate reduction rates, as published by Treude *et al.* (2005) and the influx of free sulfide from deeper sediments was equal to the total free sulfide consumption in the suboxic zone.

Biomass determination

Beggiatoa biomass was determined within 1 day after sampling. A core was sliced in 0.5–1 cm intervals, and subsamples from each interval (300–500 mg) were suspended in filtered seawater (10 ml). From 300–400 mg of this suspension, the *Beggiatoa* filaments were enumerated by microscopy. The biomass was calculated from the filament volume (cylindrical shape) assuming a density of 1 g cm^{-3} .

Cell-specific nitrate reduction and sulfide oxidation rates

Samples (0.8 ml) from the upper 3 cm of sediment were transferred into glass vials, 0.2 ml seawater was added, and the vials sealed by a rubber stopper. One vial was left open to serve as oxygenated reference. After 12, 20 and 42 days, two vials were used for intracellular nitrate, biomass and motility measurements. Cell motility, as a measure for viability, was determined from a parallel vial by microscopy. The nitrate reduction rate by *Beggiatoa* was determined from the decrease of the intracellular nitrate. Sulfide oxidation rates were calculated from the nitrate reduction rates assuming a stoichiometry $\text{H}_2\text{S}/\text{NO}_3^-$ of 1 or 4, for the oxidation to sulfate or sulfur, respectively.

Total sedimentary nitrate and elemental sulfur measurements

Sediment cores were sliced in 0.5–1 cm intervals, fixed in ZnAc (20 ml, 20% solution), frozen and thawed. Porewater was extracted by centrifugation at 3000 g for 10 min. This procedure was found to reproducibly release and extract vacuolar nitrate. Nitrite plus nitrate were measured in the supernatant with a NO_x Analyser (Thermo Environmental Instruments, Franklin, MA, USA) based on NO_3^- and NO_2^- reduction to NO by V(III)Cl₃ (in 1 M HCl) (Braman and Hendrix, 1989).

Sulfur was extracted from the pellet of the centrifuged samples with methanol (100%). Elemental sulfur, S(0), was determined by high-performance liquid chromatography (Zopfi *et al.*, 2004).

Intracellular nitrate and intracellular sulfur determination

Intracellular nitrate was measured in *Beggiatoa* filaments immediately after sectioning of the core. Filaments from the different sediment depths were transferred into artificial seawater (22‰) using a glass needle. Their length and width were determined by microscopy and the biovolume was calculated assuming a cylindrical shape. The whole procedure took about 1–2 h per sediment layer. Several filaments (7–11) of the same diameter (24 or 30 μm) were transferred into 250 μl of demineralized water and frozen at -20°C , causing cell rupture. After thawing, the samples were centrifuged (3000 g) and nitrate was measured in the supernatant as described above. On the basis of biovolume and the dilution factor, the average intracellular nitrate concentrations were determined. The remaining pellet was dried in air and the intracellular elemental sulfur grains of *Beggiatoa* were dissolved in methanol (100%) over 2–3 days. The elemental sulfur was measured as described above.

Nitrate reduction rates measured with stable isotope

From a sediment core of 10 cm diameter, the upper 2 cm that contained the *Beggiatoa* was removed. Three subcores of 2.5 cm diameter were taken from the remaining sediment. The sediment from the upper layer (0–2 cm) was split, two parts were frozen and thawed, to kill all *Beggiatoa*, and one part was left untreated. The three subcores were then topped up with 2 cm of the differently treated sediment, leaving 5 cm overlying water. Nitrification was inhibited in the untreated sediment that contained *Beggiatoa*, and in one treated core by addition of thiourea to a final concentration of 86 μM . The third core with frozen and thawed sediment, but otherwise untreated, was considered as the control. The overlying water was gently stirred and the cores were incubated in the dark. Directly after preparation of the cores, microsensor measurements of O_2 , H_2S and pH were performed, and repeated at weekly intervals. After 3 weeks 25 μM $^{15}\text{NO}_3^-$ was added to the overlying water, obtaining a total NO_3^- concentration of ca. 40 μM . The cores were left open for 24 h to allow the *Beggiatoa*, if present, to accumulate the $^{15}\text{NO}_3^-$. Then the cores were sealed to prevent escape of ^{15}N -labelled N_2 and left for another 24 h. Subsequently, the cores were sectioned in 0.5 cm intervals (0–3 cm depth) or 1 cm intervals (3–5 cm depth) into gastight Exetainers (6 ml, Labco Ltd, High Wycombe, UK) prefilled with 1 ml HgCl_2 solution (0.6%) and filled completely with demineralized water and sealed. A 1 ml headspace (helium) was introduced to the Exetainers to extract the labeled N_2 gas ($^{29}\text{N}_2$ and $^{30}\text{N}_2$) from the water phase and, after vigorous shaking of the Exetainers, injected into a gas chromatography-mass spectrometry (GC-MS; VG, Optima, ISOTECH, Middlewich, UK). The 1 ml of sample slurry extracted by the introduction of the headspace was used to determine the NO_x concentration by the NO_x analyzer, described above. To determine the fraction of the labeled intracellular NO_3^- (% $^{15}\text{NO}_3^-$ of total NO_3^-) at each depth, we transferred 2 ml of the slurry to another Exetainer, subsequently filled up with demineralized water. After the introduction of a 1 ml helium headspace, all NO_x were reduced to NO by adding 0.5 ml of TiCl_3 (Cox and Earp, 1982). This was injected into the GC-MS-injection port, reduced to N_2 by the reduction oven (copper at 650°C) and analyzed by MS. To the remaining slurry (3.5 ml), 0.5 ml of HBr was added to oxidize $^{15}\text{NH}_4^+$ to N_2 before analysis by GC-MS (Warembourg, 1993), before determination of $^{15}\text{N}_2$ by GC-MS. The efficiencies were measured with $^{15}\text{NO}_x$ and $^{15}\text{NH}_4^+$ standards. To obtain the total DNRA for each depth, the amount of produced $^{15}\text{NH}_4^+$ was divided by the ^{15}N -labeled fraction of NO_3^- . The areal nitrate consumption rates were calculated from the decrease of nitrate in the overlying water. The local DNRA was determined from the evolution of $^{15}\text{NH}_4^+$, and local denitrification from the evolution of $^{15}\text{N}_2$ in each depth interval. The areal rates of DNRA and denitrification

were then obtained by integration over depth. The biomass-specific DNRA rates for *Beggiatoa* were calculated as the ratio of the volumetric DNRA (corrected for the DNRA in the cores without *Beggiatoa*) and the volume fraction of *Beggiatoa* in the sediment.

Iron and manganese analyses

To obtain the concentrations of dissolved Fe^{2+} and solid-phase iron and manganese, one core was sliced in 1 cm depth intervals within 2 days after sampling. Porewater was extracted using a porewater press, pressurized by nitrogen. During extraction the surface of the core was constantly flushed with nitrogen. Porewater aliquots were immediately acidified and used for the spectrophotometric determination of dissolved Fe^{2+} with the Ferrozine method (Stookey, 1970). The remaining sediment was immediately frozen for later solid-phase analyses. For the determination of various solid iron phases, different iron extraction methods were applied, whereas here only the results of ascorbic acid extractions (Canfield, 1989; Ferdelman *et al.*, 1991) are shown, a method designed to extract reactive iron minerals. For each extraction, 0.4 g frozen sediment was used and the extracts were analyzed with the Ferrozine method (see above).

Solid-phase Mn(IV) concentrations were quantified by extracting 0.2 g of the sediment with the dithionite method (Canfield, 1989). The extracts were analyzed with flame atomic absorption spectrometry. All iron and manganese measurements were carried out in triplicates.

The diffusive Fe^{2+} flux was calculated from its profile using an effective diffusion coefficient of $0.52 \times 10^{-10} \text{ mol m}^{-2} \text{ s}^{-1}$, assuming OH^- as counter ion (Li and Gregory, 1974), corrected for temperature, salinity and porosity as described above.

Results

The sediments of Eckenförde Bay consisted of fine mud, with a mean porosity of 0.88 and density of 1.3 g cm^{-3} . The top 3–6 cm were dark gray, whereas the deeper sediments were black. The sediments were covered by thin white mats of a *Beggiatoa* community consisting of different size classes with diameters varying from 14 to $40 \mu\text{m}$. Although the white film covering the sediments was eye-catching, it represents only a small fraction of the benthic population, by far most of the filaments were inside the sediment (Figures 1 and 2). Most filaments had a diameter of 24 or $30 \mu\text{m}$ and were phylogenetically closely related to strains found in Limfjorden (*Beggiatoa* sp., Limfjord, Denmark) and Dangast (*Beggiatoa* sp., Dangast, Germany) (Musmann *et al.*, 2003; M Musmann, personal communication).

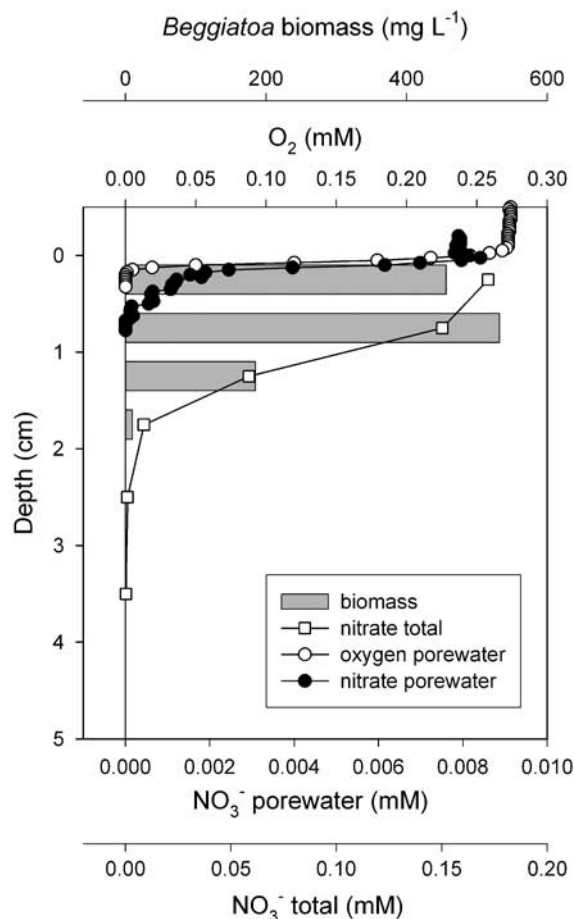


Figure 1 Profiles in Eckenförde Bay sediment measured on a retrieved core. Shown are distributions of oxygen and nitrate in porewater, measured with microsensors, total nitrate extracted from frozen and thawed sediment, and *Beggiatoa* biomass.

Biogeochemistry

In retrieved cores oxygen penetrated 0.1–0.2 cm into the sediment, and nitrate penetrated a few millimeters deeper than oxygen, as measured with microsensors (Figure 1). Sulfide was detected ($> 1 \mu\text{M}$) only below a depth of 2–6 cm (Figure 2). All measurements showed a separation between the oxic and sulfidic zone, but the width of this suboxic zone varied. In all investigated sediment cores, *Beggiatoa* was predominantly present above the sulfidic zone (Figure 2). The distribution was either bell-shaped or a gradual decrease of cell densities with depth was observed. Although occasionally living filaments were found in the sulfidic zone, free sulfide, in concentrations above $1 \mu\text{M}$, was clearly not an attractant for *Beggiatoa*. The upward sulfide flux from the sulfidic zone into the suboxic zone varied from core to core, and averaged $4.3 \text{ mmol m}^{-2} \text{ day}^{-1}$ ($\pm 2 \text{ mmol m}^{-2} \text{ day}^{-1}$).

Nitrate was measured in sediments that were Zn-treated, frozen and thawed to open vacuoles and cell membranes of the nitrate-storing organisms. These nitrate profiles strongly differed from the

nitrate profiles measured with microsensors. With microsensors only extracellular nitrate is detected. The total nitrate concentrations in *Beggiatoa*-inhabited sediments were much higher than in the overlying water, thus nitrate was actively accumulated inside the cells. The distribution of this intracellular nitrate correlated well with that of *Beggiatoa* biomass (Figure 1). Occasionally, near the sediment surface, nitrate was much higher than estimated from *Beggiatoa* abundance (Figure 3a), which indicates that other nitrate-accumulating organisms were present, probably diatoms (Lomstein et al., 1990). In that case, a good agreement between

nitrate content and *Beggiatoa* biomass could only be achieved by a procedure where *Beggiatoa* filaments were first removed from sediments, counted and their volume determined. Then they were pooled per sediment depth, and their nitrate was extracted and quantified (Figure 3a). In conclusion, the nitrate found inside the sediments below 0.3 cm depth originated entirely from *Beggiatoa* vacuoles.

In contrast to nitrate, only a small fraction of the sulfur in sediments is associated with *Beggiatoa*. Even in the zone with the highest *Beggiatoa* density, less than 10% of the sulfur is intracellular, and the distribution pattern of sulfur is clearly different

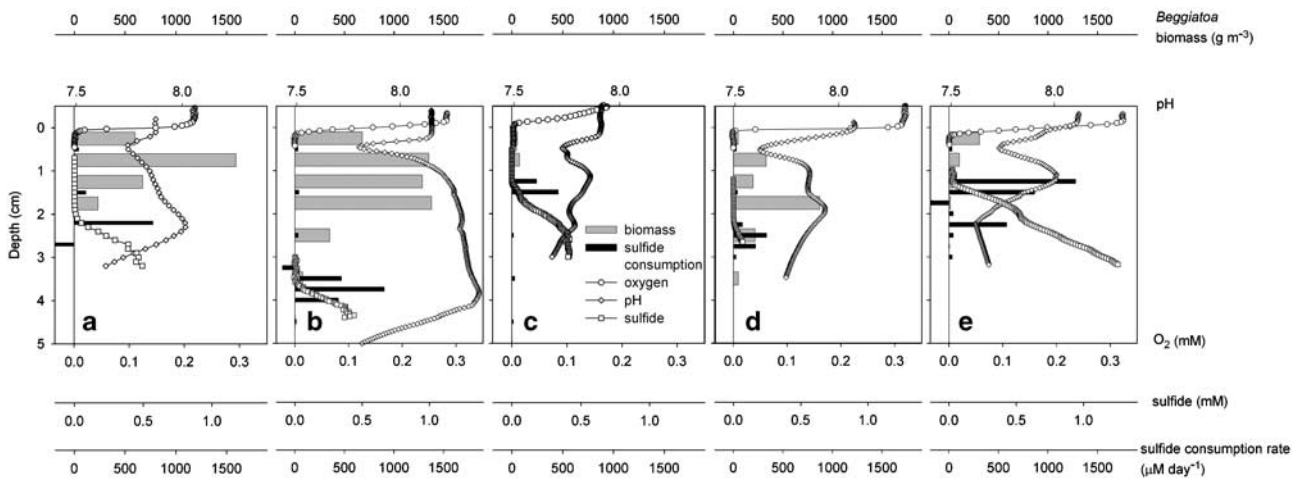


Figure 2 Distribution of *Beggiatoa* biomass, microsensors profiles of oxygen, sulfide and pH, and the rates of sulfide consumption calculated from the local sulfate reduction rates and the sulfide microprofiles. The measurements were made on retrieved cores, in (a) March 2002, (b) March 2002, (c) June 2002, (d) June 2002 and (e) January 2003.

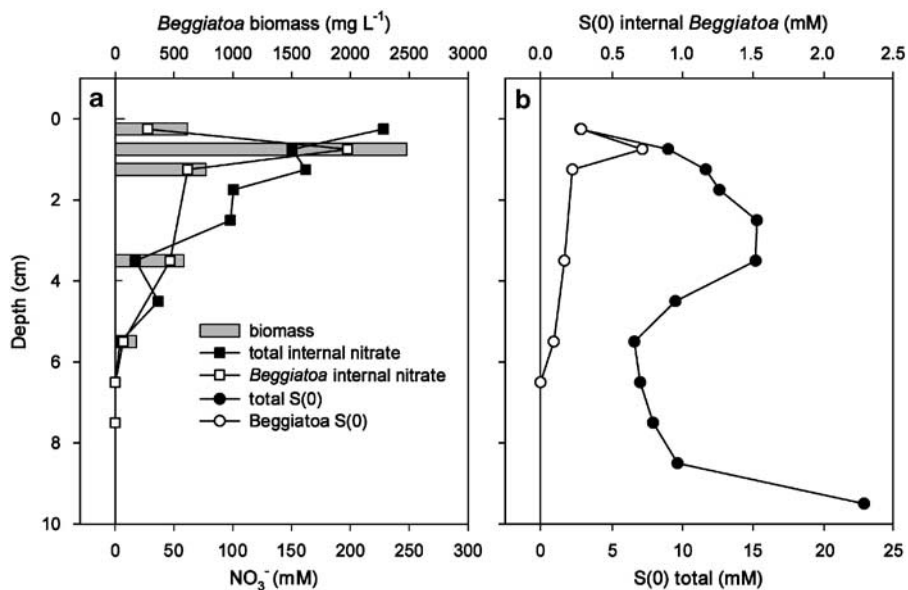


Figure 3 (a) Distribution of *Beggiatoa* biomass, total intracellular nitrate determined from frozen and thawed cores, and intracellular nitrate from *Beggiatoa*, total S(0) and intracellular S(0) from *Beggiatoa*. (b) Distribution from total sedimentary S(0) and intracellular *Beggiatoa* S(0). Observe the different scales.

from that of *Beggiatoa*. Significant sulfur pools are present below the suboxic zone (Figure 3b).

The concentration of internal nitrate was ca. 100–300 mM and the cellular sulfur content was ca. 300–400 mM (both expressed per volume of *Beggiatoa*). Thus the amount of intracellular e-donor and e-acceptor are rather well balanced, with a slight surplus towards the e-donor, for the oxidation of sulfur to sulfate ($4S(0) + 3NO_3^- + 7H_2O \rightarrow 4SO_4^{2-} + 3NH_4^+ + 2H^+$). As in the suboxic zone sulfide is supplied to the filaments continuously, most probably nitrate limits the time that filaments can reside in the sediments.

The internal stores of sulfur and nitrate allow *Beggiatoa* to live independently from external resources for up to 2 weeks, as concluded from an experiment where filaments containing 270 mM nitrate were incubated in oxygen and nitrate-free sediment. These filaments lost 70% of their intracellular nitrate in 2 weeks, and were depleted after 3 weeks, during which they remained motile. After

5 weeks the filaments were still intact, but had lost motility. The calculated mean rate of vacuolar nitrate decrease was 13 mM day^{-1} .

From experiments with stable isotope tracers ($^{15}NO_3^-$), a cell-specific DNRA rate of similar magnitude was found. The $^{15}NH_4^+$ formation coincided well with the *Beggiatoa* distribution (Figure 4a), with a local maximum at 2 cm depth. As nitrate from the overlying water does not diffuse to that depth, *Beggiatoa* must be responsible for the ammonium production and have transported the nitrate intracellularly into the sediment. This was confirmed by control experiments without *Beggiatoa*, where significant $^{15}NH_4^+$ production (DNRA) was only found near the oxic zone in the upper sediment (Figure 4b). When subtracting the NH_4^+ production of the control core from the *Beggiatoa* core, *Beggiatoa* seems not to contribute to DNRA in the upper 1 cm. The upper 1 cm of the sediments with *Beggiatoa* produced twice as much N_2 as in the controls without *Beggiatoa*. Below 1 cm depth,

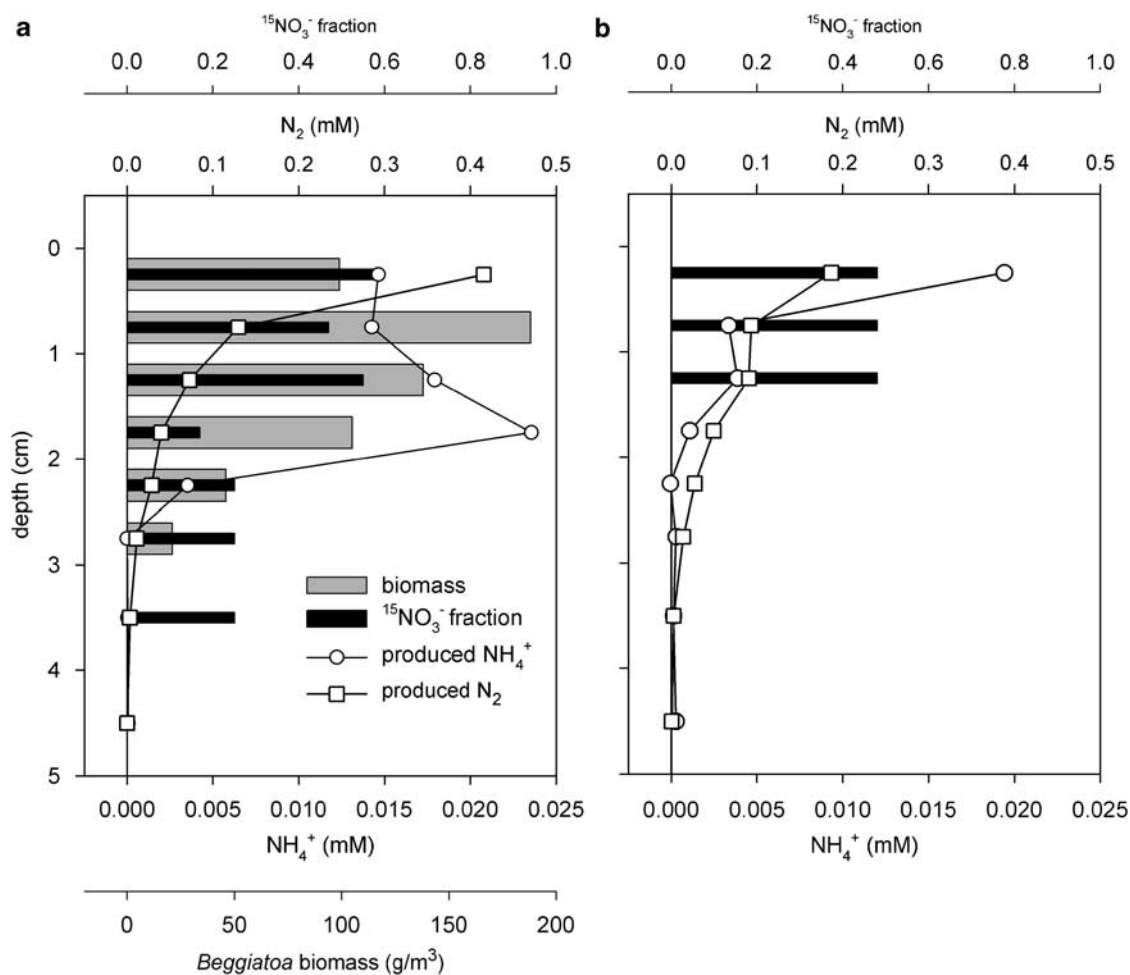


Figure 4 Results from the ^{15}N tracer experiment. (a) The distribution of *Beggiatoa* biomass, the ^{15}N -nitrate fraction of total nitrate, total produced NH_4^+ as calculated from the label fraction and produced $^{15}NH_4^+$, and produced N_2 , calculated from the label fraction and the produced $^{15}N_2$. (b) The produced NH_4^+ and N_2 in a control core without *Beggiatoa*. From the difference in NH_4^+ production between the two cores and the biomass distribution, the DNRA rates per *Beggiatoa* volume in sediments were calculated. DNRA, dissimilatory nitrate reduction to ammonium.

the depth distribution of the labeled N_2 gas was the same with or without *Beggiatoa* present. The $^{15}NO_3^-$ tracer had labeled the vacuolar nitrate pool over the full suboxic zone as can be seen from the $^{15}NO_3^-$ fraction (Figure 4a). From the specific labeling intensity and the $^{15}NH_4^+$ production rate, the total NH_4^+ production rate was calculated. The areal DNRA rate was $43 \mu\text{mol m}^{-2} \text{day}^{-1}$ in a sediment with $3 \text{ g } Beggiatoa \text{ m}^{-2}$. Assuming $1 \text{ ml of } Beggiatoa$ per g biomass , this DNRA rate is equivalent to 14 mM day^{-1} of vacuolar nitrate concentration decrease. The same results were obtained in two replicate stable isotope experiments.

The pH profiles in retrieved cores showed a local minimum at a depth of ca. 0.5–1 cm, and a clear local maximum near the top of the sulfidic zone, that is the zone where upwardly diffusing sulfide disappeared (Figures 2a–e).

The *in situ* profiles showed an oxygen penetration depth of 0.1–0.2 cm, and a sulfidic zone below ca. 10 cm depth (Figure 5). The sulfide levels peaked between 20 and 30 cm depth, reaching ca. 7 mM, and below 30 cm the concentration decreased. The pH profiles showed a minimum value at ca. 6 cm depth, and a maximum value at the top of the sulfidic zone. The separation between the oxic and sulfidic zone was much larger than observed in retrieved cores. During the *in situ* measurements, strong winds ($40\text{--}50 \text{ km h}^{-1}$) possibly caused turbulences at the seafloor and disturbance of the top sediments. Also, ship movement might have caused rough positioning on the seafloor causing replacement of sediment, and covering of the sediments below the profiler. Nevertheless, the pH profiles peaked at the top of the sulfidic zone and showed a local minimum in the suboxic zone, similar to the retrieved cores.

Solid-phase iron and manganese species had increased concentrations in the upper sediment (Figure 6). Dissolved porewater Fe^{2+} was elevated in the top 2 cm, with a local maximum of ca. $130 \mu\text{M}$ at 1 cm depth. It was lower ($<50 \mu\text{M}$) in the oxic zone, obviously due to oxidation with oxygen, and close to 0 below 2 cm depth, probably due to precipitation with free sulfide. The ascorbate extractable Fe(III) had increased concentrations up to 30 mM in the top 4 cm. In principle, the method extracts also some of the FeS pool; however, the independent extraction of FeS only showed insignificant amounts. Manganese extracted with dithionite peaked in the upper centimeter with 3 mM, about three times the background level found below.

Effects of nitrate, oxygen and sulfide

To investigate the distinct pH profiles, we tested the hypothesis that the local pH minimum in the suboxic zone was caused by aerobic oxidation of sulfur to sulfate, a process well known to reduce the pH value. The oxygen in the overlying water was experimentally reduced to $<40 \mu\text{M } O_2$ by flushing

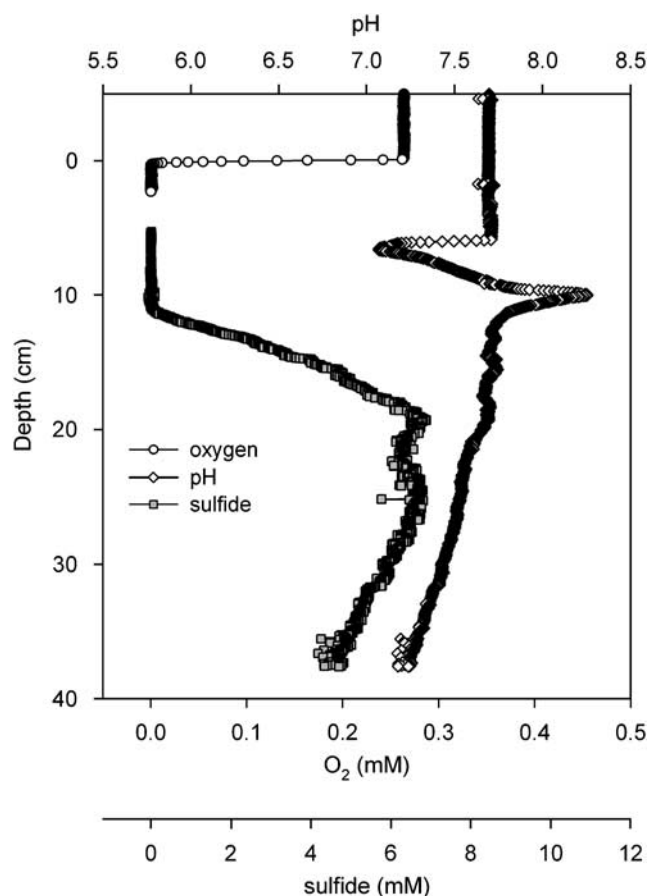


Figure 5 Microprofiles of oxygen, sulfide and pH measured *in situ* with microsensors mounted on an autonomous profiler. The sediment surface was determined as the depth with the steepest oxygen concentration gradient.

with argon, for a period of 6 h. The penetration depth of oxygen became close to 0. The only effect on pH was a slight increase in the overlying water due to CO_2 outgassing, but the local pH minimum remained unchanged (Figure 7a), thus it was concluded that the local pH minimum was not related to an oxygen-dependent process. Also the addition of $200 \mu\text{M}$ nitrate (10-fold the *in situ* concentration) to the overlying water did not change the pH profile in the sediment (Figure 7b), suggesting that also nitrate respiration did not cause the pH minimum.

To investigate the possibility that the local pH maximum at the top of the sulfidic zone was caused by interaction of free sulfide with oxidized compounds in the sediment, 0.3 mM sulfide was added to the overlying water. This resulted in an immediate increase in the pH in the upper zone of the sediment, to which sulfide could penetrate (Figure 8). The pH reached a maximum value of 9.5. The sediment surface turned instantly black, indicating FeS formation. Overnight the sulfide disappeared and the pH profile recovered to the original shape.

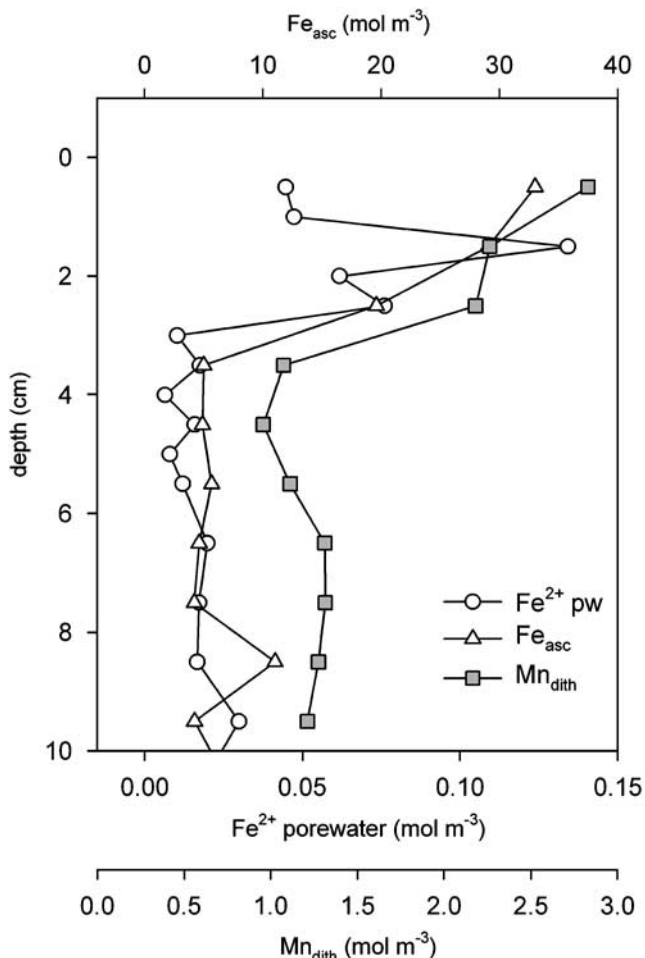


Figure 6 Distributions of dithionite extracted manganese (Mn_{dith}), Fe^{2+} dissolved in the porewater, and ascorbic acid extractable sedimentary iron (Fe_{asc}), which is regarded as the most reactive Fe(III) fraction.

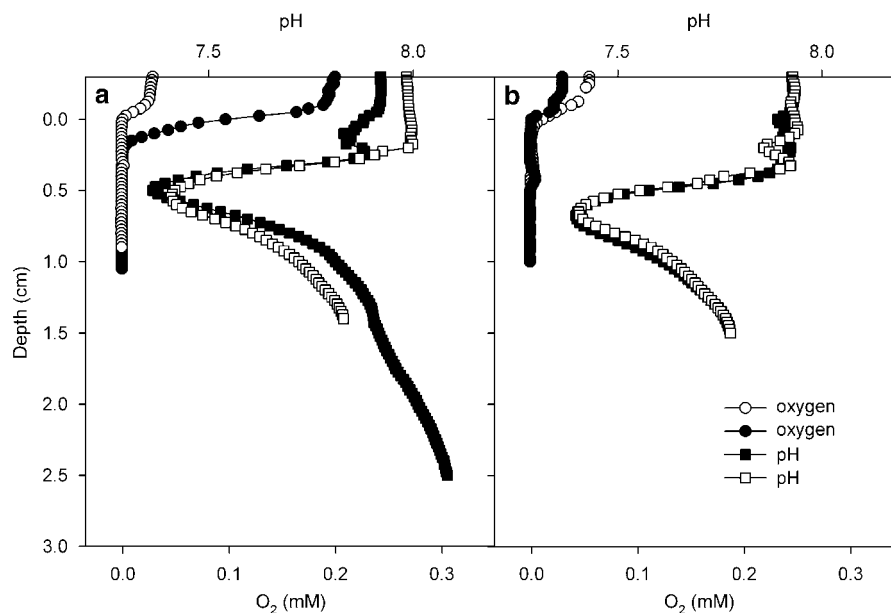


Figure 7 The effect of (a) oxygen decrease and (b) addition of $200 \mu M$ nitrate on the subsurface pH profile, measured with microsensors. Closed symbols indicate profiles before treatment, open symbols represent the situation 6–8 h after the change. Oxygen or nitrate have no effect on the pH profiles.

Discussion

The *in situ* and *ex situ* microsensor measurements all showed a clear separation between the sulfidic and the oxic zone, and a local pH maximum at the top of the sulfidic zone. The *in situ* profile has a larger suboxic zone between the oxic and sulfidic zone than those measured on retrieved cores. This indicates that before or during the *in situ* deployment of the microsensor profiler sediment was deposited in the area of profiling, either by wind-driven bottomwater currents or by the deployment of the equipment. This changed the oxygen distribution, but the local pH in the upper 3 cm remained that of seawater. Also irregular topography can lead to an overestimation of the suboxic zone. The local pH maximum at the top of the sulfidic zone and the local minimum below the oxic zone were observed both *in situ* and in the retrieved cores. Thus the characteristic local pH maximum and minimum in the profiles were not an artifact of the retrieval.

Our observations show that *Beggiatoa* is predominantly distributed in the suboxic and oxic zone, and avoids the sulfidic zone. Sulfide enters the suboxic *Beggiatoa* zone by local sulfate reduction and by diffusion upwards from the sulfidic zone. Our *in situ* microprofiles showed a sulfide maximum between 25 and 35 cm depth. At this depth the sulfate to methane transition zone is found, and the highest rates of anaerobic oxidation to methane (Treude *et al.*, 2005). From the sulfide oxidation rates calculated for *Beggiatoa*, the published local sulfate reduction rates that were measured at the same stations (Treude *et al.*, 2005), and the calculated sulfide influx, we obtained a budget for the suboxic zone and estimated the importance of

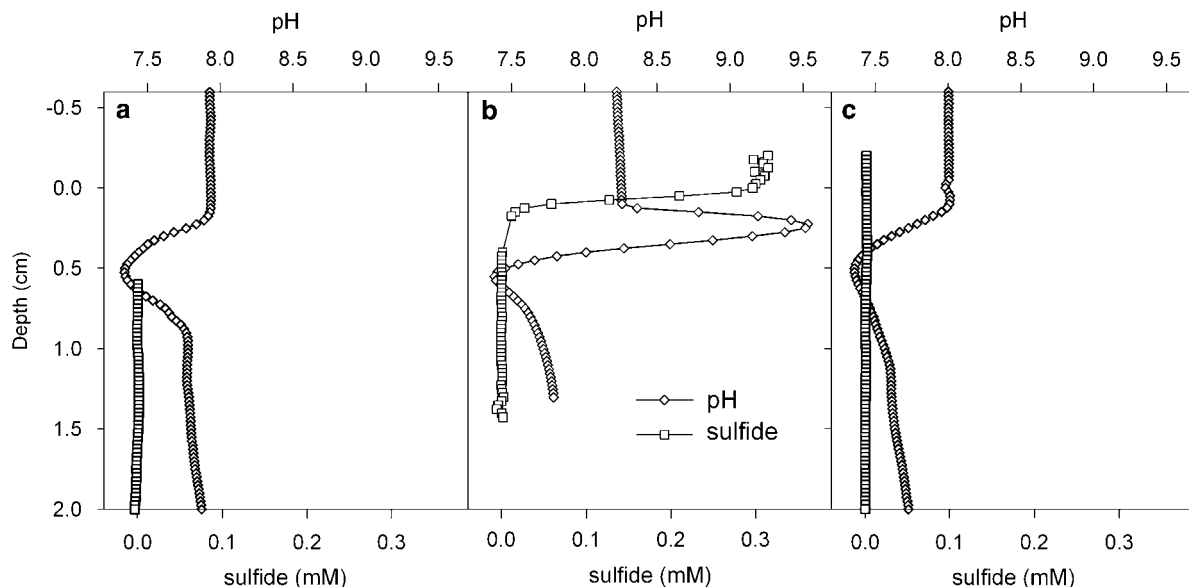
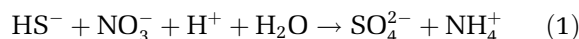
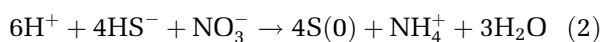


Figure 8 Effect of sulfide addition to the overlying water on the pH profile. The experiment was done under reduced oxygen, by flushing with argon. (a) Before addition, (b) 10 min after addition, (c) 8 h after addition.

Beggiatoa for sulfide oxidation (Table 1). The biomass-specific DNRA was found to be ca. 13–14 mm day⁻¹ close to values previously found for *Thioploca* (Otte *et al.*, 1999). Thus the biomass-specific sulfide oxidation rate of *Beggiatoa* is ca. 13 mm day⁻¹, when sulfide is oxidized to sulfate:



or ca. 52 mm day⁻¹ for the first step in sulfide oxidation to elemental sulfur:



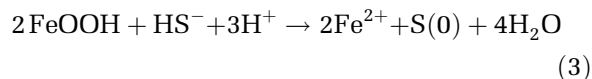
Combining the estimated biomass-specific conversion rate (13 mm day⁻¹) and the measured biomass quantities (Figure 2), the areal rates of sulfide oxidation to sulfate by *Beggiatoa* were estimated to vary between 0.0086 and 0.38 mmol m⁻² day⁻¹, averaging 0.16 ± 0.15 mmol m⁻² day⁻¹. The actual sulfide oxidation rate during balanced growth, when all sulfides are oxidized to sulfates, will be slightly higher, as a part of the reducing power is used for cell growth. Therefore, per mol of nitrate ca. 1.2 mol of sulfide can be oxidized to sulfate, if the growth yield with nitrate is the same as with oxygen (Nelson *et al.*, 1986).

The budget calculation (Table 1) shows that only a small fraction of the sulfide input into the suboxic zone is oxidized by *Beggiatoa*, as the influx and local production far exceeds the estimated nitrate reduction rate. Even if we assume that sulfide oxidation locally stops at the level of sulfur (Sayama *et al.*, 2005), allowing four sulfides to be oxidized with one nitrate, *Beggiatoa* activity is insignificant for the total sulfide oxidation. The sulfide input into the suboxic zone was mostly the influx from deeper sediments, and was consumed at the interface of the

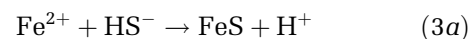
Table 1 S-budget of the suboxic zone inhabited by *Beggiatoa* (upper 2 cm)

Sulfide input (mmol m ⁻² day ⁻¹)		Sulfide consumption (mmol m ⁻² day ⁻¹)	
Diffusion from sulfidic zone	Local sulfate reduction	<i>Beggiatoa</i>	Inferred chemical oxidation
4.3 (±2) (86%)	0.7 (14%)	0.16 (±0.15) (3%)	4.84 (97%)

sulfidic zone and the suboxic zone, causing the local maximum in sulfide consumption (Figure 2). This distribution of sulfide consumption rates did not correlate with the distribution of *Beggiatoa* (Figure 2). Whereas *Beggiatoa* consumed ca. 20% of the sulfide produced by sulfate reduction in the suboxic zone, almost all of the influx from deeper sediments must be consumed by chemical oxidation. The most likely electron acceptor for such anaerobic sulfide oxidation is Fe(III).



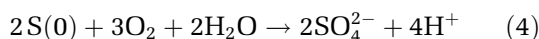
A part of the soluble reduced iron and sulfide will form iron sulfides



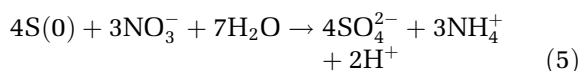
Whereas the first reaction involves dissipation of protons and thus a pH increase, the second step leads to a small pH decrease. In a gradient system, the second step is not 100% efficient, and a part of the Fe²⁺ escapes into the suboxic zone, where its

concentration is indeed elevated (Figure 6). This mechanism is corroborated by the local pH maximum consistently found at the interface between the suboxic zone and the sulfidic zone (Figure 2). The product of sulfide oxidation by Fe(III) is elemental sulfur, which is indeed abundantly found in the sediments (Figure 3b).

The local pH minimum near the surface was very stable (Figures 7 and 8), which also points to a chemical process. The local pH minimum was not influenced by oxygen or nitrate (Figure 7), making a biological oxidation process unlikely:

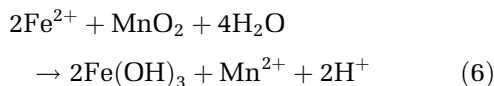


or



Also aerobic iron oxidation cannot explain the pH profile, as the pH minimum was always below the oxic zone, and not affected by oxygen levels in the water phase.

In the absence of oxygen, Fe^{2+} may rapidly be oxidized by manganese oxides (Postma, 1985), which leads to a pH decrease:

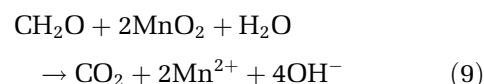
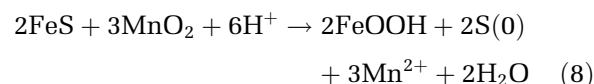
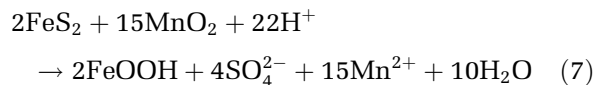


The analyses of sedimentary iron and manganese support these hypotheses (Figure 6). Elevated amounts of oxidized iron were found in the upper 3 cm, and were thus available for sulfide oxidation. The iron minerals in the upper sediment were very reactive, as shown by the experimental sulfide addition to the overlying water (Figure 8). Sulfide penetration into the upper sediment was limited, and an immediate very strong pH increase was observed. Below 3 cm depth low levels of Fe(III) were found, which were probably less reactive. Also a clear elevation of manganese was found in the upper 3 cm, including the oxic zone. The manganese extracted with dithionite is thought to be the reactive pool, and the elevated levels in the upper sediments is dominated by Mn(IV) (Kostka and Luther, 1994).

The steep Fe^{2+} peak indicates strong Fe(III)-driven mineralization in the suboxic zone. The Fe^{2+} is produced just below or in the Mn(IV)-rich layer, and we propose that it is the Fe^{2+} oxidation by MnO_2 which leads to the observed pH minimum below the oxic zone. The reaction of Eq. 6 is not instant, but proceeds on a timescale of hours (Postma, 1985), thus indeed free Fe^{2+} can be present at detectable levels in Mn(IV)-containing sediments. If the effective diffusion coefficient for Fe^{2+} is $0.52 \times 10^{-9} \text{ m}^2 \text{ s}^{-1}$, 3 mM of MnO_2 in the upper 1 cm is sufficient to absorb the Fe^{2+} diffusing upwards from its peak for several weeks. This solid-phase electron acceptor for iron oxidation might also explain why the local pH minimum was observed

in the *in situ* profiles at 6 cm depth (Figure 5): the MnO_2 -containing layer had been covered with reduced mud, but was not yet depleted.

Other MnO_2 reduction processes lead to pH increase, for example when coupled to the oxidation of FeS or FeS_2 or to organic compounds:



These processes are thought to be partly microbially catalyzed (Schippers and Jørgensen, 2001). Because no pH increase was observed in the upper sediment, however, they were apparently not dominant.

Thus, the pH profiles can be explained from manganese and iron cycling, and the metal cycling drives the oxidative sulfur cycling. Frequent resuspension and bioturbation is needed for intense iron and manganese cycling in muddy sediments (Canfield *et al.*, 2005). The upper layer of the sediment is, possibly due to storms or methane ebullition (Roden and Wetzel, 1996), regularly resuspended in the aerated bottom water leading to oxidation of Mn^{2+} and Fe^{2+} . Irregular resuspension of upper sediment layers was considered to explain the presence of potentially active aerobic methanotrophs in the upper 5 cm (Treude *et al.*, 2005). Bioventilation and bioturbation may be less important for the oxidation of reduced iron and manganese, as signs of bioturbation were found in the upper centimeter only (Treude *et al.*, 2005).

The oxidized layer can be 10 cm thick as observed *in situ*, but is more often 2–4 cm thick. This layer, in the sediments we investigated, is the habitat for *Beggiatoa*. As summarized in Figure 9, sulfide diffusing from below into this layer is rapidly oxidized by Fe(III), forming a steep sulfide gradient and a local maximum in pH. Fe^{2+} diffuses upwards and reaches the MnO_2 rich zone, where it is oxidized, leading to a local minimum in pH.

Whereas we conclude that most sulfide is oxidized through chemical processes, a recent study (Sayama *et al.*, 2005) came to the opposite conclusion that the observed pH microprofiles and sulfide oxidation must be explained by the metabolic activities of *Beggiatoa*. Their study was done in *Beggiatoa* mats transplanted experimentally on sulfidic sediments. The authors explained the local pH maximum at the upper sulfidic zone by the oxidation of sulfide by nitrate to S(0) (Eq. 1), and the local pH minimum by the aerobic oxidation of S(0)

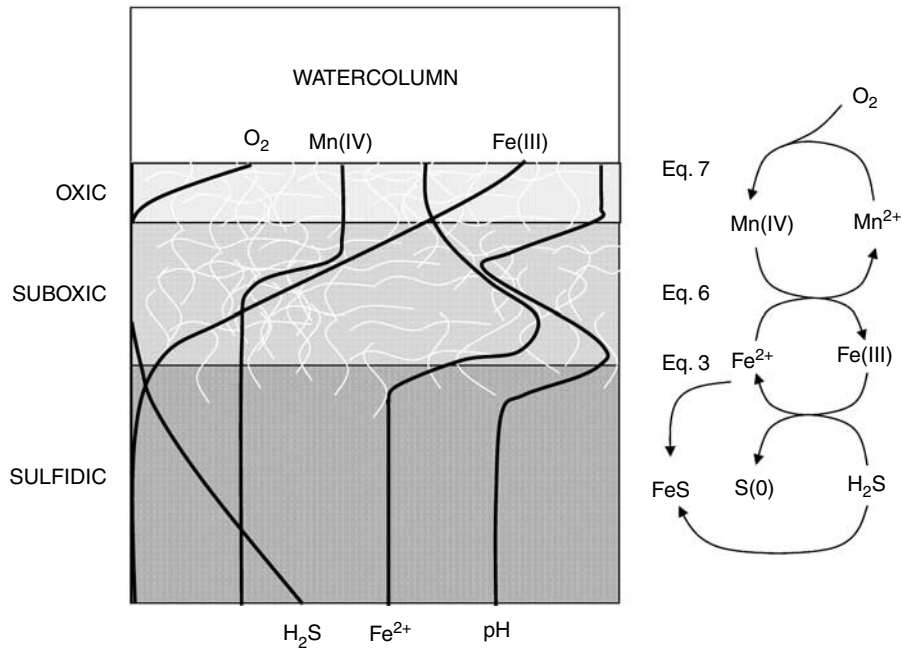


Figure 9 Overview of the main geochemical reactions in the oxic (dashed), suboxic (light gray) and sulfidic (dark gray) zones, and the schematic porewater profiles. The profiles are not quantitative. The distribution of *Beggiatoa* is indicated by the white filaments.

to sulfate (Eq. 4). The sulfide fluxes we calculated from their published profiles are four- to fivefold lower than their measured DNRA rates (which were very high and entirely attributed to *Beggiatoa*), implying that DNRA could easily oxidize all sulfide diffusing upwards to sulfate (Eq. 1). The differences could be explained by a *Beggiatoa* density that was much higher than in our study; however, cell densities were not reported.

Why is *Beggiatoa* so abundant in the studied sediment? A prerequisite for *Beggiatoa* is a highly porous sediment (Jørgensen, 1977), like indeed the sediments in this study. The sulfate reduction rate in the zone where *Beggiatoa* occurs was comparable to rates found in temperate intertidal sediments, in subtidal sediments, and in many other sediments (Canfield *et al.*, 2005), where, however, no conspicuous *Beggiatoa* mats were found. Thus the abundance of *Beggiatoa* in the sediments studied here cannot be explained by a high volumetric sulfate reduction rate, as in other sediments without *Beggiatoa* similar rates were found. The pH in the sediments we investigated was between 7 and 8, a typical marine sediment value (Boehme *et al.*, 1998). In summary, in the suboxic zone where *Beggiatoa* resides we could not detect unique characteristics that could explain the presence of *Beggiatoa*. One distinguishing characteristic of habitats where *Beggiatoa* is found appears to be the presence of detectable free sulfide. Typical habitats include cold seeps (Barry *et al.*, 1996; Kalanetra *et al.*, 2003), upwelling areas with high organic input (Brüchert *et al.*, 2003), whale carcasses, sulfidic springs (Martinez *et al.*, 1997; Mattison *et al.*, 1998),

hydrothermal vents (Nelson *et al.*, 1989) and hypersaline mats (Garcia-Pichel *et al.*, 1994; Jonkers *et al.*, 2003), all of which have steep sulfide gradients. High temperatures seem to exclude *Beggiatoa* as they are not reported from sulfidic hot springs. In principle, a suboxic zone is not essential, because also when sulfidic and oxic zones overlap *Beggiatoa* can persist and develop a mat on the surface (Jørgensen and Revsbech, 1983). In our studies, the sulfide diffusing upwards was scavenged by Fe(III), thus this source reached only the very small fraction of the *Beggiatoa* population that is present at the sulfidic interface. Therefore, sulfide diffusing from below the suboxic zone could not insignificantly feed the *Beggiatoa* population in the suboxic zone. The amount of sulfide produced locally was sufficient for their metabolic needs, and they had a sufficiently high affinity for H₂S to compete with the chemical oxidation processes. Although most of the *Beggiatoa* reside in the suboxic zone, where sulfide concentrations were low ($\leq 1 \mu\text{M}$), sulfide may not be very toxic for *Beggiatoa*. Occasionally, filaments were found deep in the sulfidic zone, and despite high sulfide concentrations, they were motile. However, generally the sulfidic zone is avoided.

We propose that *Beggiatoa* needs a steep sulfide gradient for orientation. Owing to their internal stores of sulfur and nitrate they can travel independent from external supplies for a period of days to weeks. With a gliding velocity of $2 \mu\text{m s}^{-1}$ (Nelson *et al.*, 1989), their linear path length is 70 cm in 4 days if the vacuolar nitrate concentration is 50 mM, and even 5 m in 3 weeks when they start the journey

with the highest measured nitrate concentration of 370 mM. When moving in random direction in sediments without a signal to return to the surface, the cells would sooner or later reach depths in the sediments from which they cannot return to the oxidized zone before their stored nitrate is depleted. A steep sulfide gradient could provide a signal to return. Indeed, we observed a phobic response to sulfide in the *Beggiatoa* mats from the Håkon Mosby mud volcano, a cold seep in the Barents Sea. When 2 cm thick agar plugs containing 3 mM sulfide (pH 7.8) were inserted into *Beggiatoa* mats, filaments cleared a ring of several millimeters wide around the plug within hours. No repulsion was observed with sulfide-free controls (data not shown). A vacuolated nitrate storing hypersaline *Beggiatoa* strain was repelled by sulfide, as shown in sulfide gradient tubes (Susanne Hinck, personal communication). Several authors have alluded to a phobic response by *Beggiatoa* to sulfide (for example, Garcia-Pichel *et al.*, 1994; Canfield *et al.*, 2005), but it is not yet properly documented. More detailed investigations are needed towards the negative tactile response towards sulfide, for example it is not known how steep the gradient should be to function as repellent, and at which concentrations sulfide may become toxic for *Beggiatoa*. Random motion in a narrow zone between the surface and the steep sulfide gradient would allow *Beggiatoa* to reach the surface with a sufficient frequency to reload the vacuole with nitrate. Consequently, the negative tactile response towards sulfide allows them to persist and thrive in anoxic sediments. The special ecological niche for large nitrate storing *Beggiatoa* is thus not explained by substrate supply, thermodynamics or kinetic options, but by behavior.

Acknowledgements

We thank our colleagues Tim Ferdelman, Tina Treude and Susanne Hinck for valuable comments, and our technicians Gaby Eickert, Ines Schroeder, Karin Hohmann for supply of excellent microsensors and assistance during the measurements. Else Wieringa is acknowledged for the nitrate measurements. We thank Wolfgang Queisser (IfM-GEOMAR) for his generous hospitality and for using his workshop as laboratory. We thank the crew of the Litorina (IfM-GEOMAR) for the sampling and help with deployments. The study is supported by the Bundesministerium für Bildung und Forschung and the Deutsche Forschungsgemeinschaft in the frame of the GEOTECHNOLOGIEN project MUMM (FKZ G0554A, 03G0608A) and the Max-Planck-Institute for Marine Microbiology.

References

Ahmad A, Barry JP, Nelson DC. (1999). Phylogenetic affinity of a wide, vacuolated, nitrate-accumulating *Beggiatoa* sp. from Monterey Canyon, California, with *Thioploca* spp. *Appl Environ Microbiol* **65**: 270–277.

- Barnett PRO, Watson J, Connelly D. (1984). A multiple corer for taking virtually undisturbed samples from shelf, bathyal and abyssal sediments. *Oceanologica Acta* **7**: 399–408.
- Barry JP, Greene HG, Orange DL, Baxter CH, Robison BH, Kochevar RE *et al.* (1996). Biologic and geologic characteristics of cold seeps in Monterey Bay, California. Deep Sea Research Part I. *Oceanogr Res Pap* **43**: 1739–1762.
- Berner RA. (1981). A new geochemical classification of sedimentary environments. *J Sed Petrol* **51**: 359–365.
- Boehme SE, Sabine CL, Reimers CE. (1998). CO₂ fluxes from a coastal transect: a time-series approach. *Mar Chem* **63**: 49–67.
- Braman RS, Hendrix SA. (1989). Nanogram nitrite and nitrate determination in environmental and biological-materials by Vanadium(III) reduction with chemiluminescence detection. *Anal Chem* **61**: 2715–2718.
- Brüchert V, Jørgensen BB, Neumann K, Riechmann D, Schlösser M, Schulz HN. (2003). Regulation of bacterial sulfate reduction and hydrogen sulfide fluxes in the central Namibian coastal upwelling zone. *Geochim Cosmochim Acta* **67**: 4505–4518.
- Canfield D, Thamdrup B, Kristensen E. (2005). *Aquatic Geomicrobiology*. Elsevier AP: Amsterdam, the Netherlands.
- Canfield DE. (1989). Reactive iron in marine sediments. *Geochim Cosmochim Acta* **53**: 619–632.
- Cox RD, Earp RF. (1982). Determination of trace level organics in ambient air by high-resolution gas chromatography with simultaneous photoionization and flame ionization detection. *Anal Chem* **54**: 2265–2270.
- de Beer D. (2000). Potentiometric microsensors for *in situ* measurements in aquatic environments. In: Buffle J, Horvai G (eds). *In situ Monitoring of Aquatic Systems: Chemical Analysis and Speciation*. Wiley & Sons: Chichester, UK. pp 161–194.
- de Beer D, Sauter E, Niemann H, Kaul N, Foucher JP, Witte U *et al.* (2006). *In situ* fluxes and zonation of microbial activity in surface sediments of the Håkon Mosby Mud Volcano. *Limnol Oceanogr* **51**: 1315–1331.
- Ferdelman TG, Church TM, Luther GWI. (1991). Sulfur enrichment of humic substances in a Delaware salt marsh sediment core. *Geochim Cosmochim Acta* **55**: 979–988.
- Ferdelman TG, Lee C, Pantoja S, Harder J, Bebout B, Fossing H. (1997). Sulfate reduction and methanogenesis in a *Thioploca*-dominated sediment off the coast of Chile. *Geochim Cosmochim Acta* **61**: 3065–3079.
- Fossing H, Gallardo VA, Jørgensen BB, Huettel M, Nielsen LP, Schulz H *et al.* (1995). Concentration and transport of nitrate by the mat-forming sulphur bacterium *Thioploca*. *Nature* **374**: 713–715.
- Froelich PN, Klinkhammer GP, Bender ML, Luedtke NA, Heath GR, Cullen D *et al.* (1979). Early oxidation of organic matter in pelagic sediments of the eastern equatorial Atlantic: suboxic diagenesis. *Geochim Cosmochim Acta* **43**: 1075–1090.
- Garcia-Pichel F, Mechling M, Castenholz RW. (1994). Diel migrations of microorganisms within a benthic, hypersaline mat community. *Appl Environ Microbiol* **60**: 1500–1511.
- Gieseke A, de Beer D. (2004). Use of microelectrodes to measure *in situ* microbial activities in biofilms, sediments, and microbial mats. In: Akkermans ADL, van Elsas D (eds). *Molecular Microbial Ecology*

- Manual*. Kluwer: Dordrecht, the Netherlands, pp 1581–1612.
- Jeroschewski P, Steukart C, Kühl M. (1996). An amperometric microsensor for the determination of H₂S in aquatic environments. *Anal Chem* **68**: 4351–4357.
- Jonkers HM, Ludwig R, De Wit R, Pringault O, Muyzer G, Niemann H *et al.* (2003). Structural and functional analysis of a microbial mat ecosystem from a unique permanent hypersaline inland lake: ‘La Salada de Chiprana’ (NE Spain). *FEMS Microbiol Ecol* **44**: 175–189.
- Jørgensen BB. (1977). Distribution of colorless sulfur bacteria (*Beggiatoa* spp.) in a coastal marine sediment. *Mar Biol* **41**: 19–28.
- Jørgensen BB, Revsbech NP. (1983). Colorless sulfur bacteria, *Beggiatoa* spp. and *Thiovulum* spp. in O₂ and H₂S microgradients. *Appl Environ Microbiol* **45**: 1261–1270.
- Kalanetra KM, Nelson DC, Joye SB. (2003). Evolutionary relationships of novel, vacuolate, sulfur-oxidizing bacteria from hydrothermal vents and cold seeps. *Abstracts of the General Meeting of the American Society for Microbiology* **103-N**: 362.
- Kostka JE, Luther GW. (1994). Partitioning and speciation of solid-phase iron in salt-marsh sediments. *Geochim Cosmochim Acta* **58**: 1701–1710.
- Larsen LH, Kjaer T, Revsbech NP. (1997). A microscale NO₃⁻ biosensor for environmental applications. *Anal Chem* **69**: 3527–3531.
- Li Y-H, Gregory S. (1974). Diffusion of ions in sea water and deep-sea sediments. *Geochim Cosmochim Acta* **38**: 703–714.
- Lomstein E, Jensen MH, Sorensen J. (1990). Intracellular NH₄⁺ and NO₃⁻ pools associated with deposited phytoplankton in a marine sediment (Aarhus Bight, Denmark). *Mar Ecol Prog Ser* **61**: 97–105.
- Martinez A, Pibernat I, Figueras J, Garcia-Gil J. (1997). Structure and composition of freshwater microbial mats from a sulfur spring (“Font Pudosa”, NE Spain). *Microbiologia* **13**: 45–56.
- Mattison RG, Abbiati M, Dando PR, Fitzsimons MF, Pratt SM, Southward AJ *et al.* (1998). Chemoautotrophic microbial mats in submarine caves with hydrothermal sulphidic springs at Cape Palinuro, Italy. *Microb Ecol* **35**: 58–71.
- McHatton S, Barry JP, Jannasch HW, Nelson DC. (1996). High nitrate concentrations in vacuolate autotrophic marine *Beggiatoa* spp. *Appl Environ Microbiol* **62**: 954–958.
- Millero FJ, Plese T, Fernandez M. (1988). The dissociation of hydrogen sulfide in seawater. *Limnol Oceanogr* **33**: 269–274.
- Mussmann M, Schulz HN, Strotmann B, Kjaer T, Nielsen LP, Rossello-Mora RA *et al.* (2003). Phylogeny and distribution of nitrate-storing *Beggiatoa* spp. in coastal marine sediments. *Environ Microbiol* **5**: 523–533.
- Nelson DC, Jørgensen BB, Revsbech NP. (1986). Growth pattern and yield of a chemoautotrophic *Beggiatoa* sp. in oxygen-sulfide microgradients. *Appl Environ Microbiol* **52**: 225–233.
- Nelson DC, Wirsén CO, Jannasch HW. (1989). Characterization of large, autotrophic *Beggiatoa* spp. abundant at hydrothermal vents of the Guaymas Basin. *Appl Environ Microbiol* **55**: 2909–2917.
- Otte S, Kuenen JG, Nielsen LP, Paerl HW, Zopfi J, Schulz HN *et al.* (1999). Nitrogen, carbon, and sulfur metabolism in natural Thioploca samples. *Appl Environ Microbiol* **65**: 3148–3157.
- Postma D. (1985). Concentrations of Mn and separation of Fe in sediments. 1. Kinetics and stoichiometry of the reaction between birnessite and dissolved Fe(II) at 10°C. *Geochim Cosmochim Acta* **49**: 1023–1033.
- Revsbech NP. (1989). An oxygen microelectrode with a guard cathode. *Limnol Oceanogr* **55**: 1907–1910.
- Roden EE, Wetzel RG. (1996). Organic carbon oxidation and suppression of methane production by microbial Fe(III) oxide reduction in vegetated and unvegetated wetland sediments. *Limnol Oceanogr* **41**: 1733–1748.
- Sayama M. (2001). Presence of nitrate-accumulating sulfur bacteria and their influence on nitrogen cycling in a shallow coastal marine sediment. *Appl Environ Microbiol* **67**: 3481–3487.
- Sayama M, Risgaard-Petersen N, Nielsen LP, Fossing H, Christensen PB. (2005). Impact of bacterial NO₃⁻ transport on sediment biogeochemistry. *Appl Environ Microbiol* **71**: 7575–7577.
- Schippers A, Jørgensen BB. (2001). Oxidation of pyrite and iron sulfide by manganese dioxide in marine sediments. *Geochim Cosmochim Acta* **65**: 915–922.
- Schulz HN, Brinkhoff T, Ferdelman TG, Hernandez Marine M, Teske A, Jørgensen BB. (1999). Dense populations of a giant sulfur bacterium in Namibian shelf sediments. *Science* **284**: 493–495.
- Schulz HN, Jørgensen BB. (2001). Big bacteria. *Ann Rev Microbiol* **55**: 105–137.
- Stookey LL. (1970). Ferrozine – a new spectrophotometric reagent for iron. *Anal Chem* **42**: 779–785.
- Treude T, Krüger M, Boetius A, Jørgensen BB. (2005). Environmental control on anaerobic oxidation of methane in the gassy sediments of Eckenfoerde Bay (German Baltic). *Limnol Oceanogr* **50**: 1771–1786.
- Ullman WJ, Aller RC. (1982). Diffusion coefficients in nearshore marine sediments. *Limnol Oceanogr* **27**: 552–556.
- Vargas A, Strohl WR. (1985). Utilization of nitrate by *Beggiatoa alba*. *Arch Microb* **142**: 279–284.
- Warembourg F. (1993). Nitrogen fixation in soil and plant systems. In: Paul E, Melillo J, Knowles R, Blackburn H (eds). *Nitrogen Isotope Techniques*. Elsevier: Amsterdam, the Netherlands, pp 127–156.
- Wenzhöfer F, Holby O, Glud RN, Nielsen HK. (2000). *In situ* microsensor studies of a shallow hydrothermal vent at Milos, Greece. *Mar Chem* **69**: 43–54.
- Zopfi J, Ferdelman TG, Fossing H. (2004). Distribution and fate of sulfur intermediates – sulfite tetrathionate, thiosulfate, and elemental sulfur – in marine sediments. In: Amend J, Edwards K, Lyons T (eds). *The Biogeochemistry of Sulfur*. GSA Special Paper. Geol. Soc. America: London, UK, pp 97–116.